# Flow and Turbulence over an Estuarine Dune – Large-Scale Flume Experiments

*Christina Carstensen*[1] *and Ingrid Holzwarth*[1]

[1] *Federal Waterways Engineering and Research Institute, christina.carstensen@baw.de*

## Summary

Bedforms, such as dunes, are found in large parts of estuaries and coastal areas. Dunes influence hydrodynamics and sediment transport in the flowing water by causing flow resistance, whereby flow energy is dissipated. The characteristics of flow over dunes are complex and vary depending on the dune shape. They have rarely been studied for estuarine dunes in particular, although a precise knowledge of the hydrodynamic processes is important, e.g. for a correct representation or parameterization in mathematical hydrodynamic models. Therefore, we conducted the first flume experiments over a typical estuarine dune. The experimental setup allowed for studying flow over a dune on a large scale and in a high level of detail. High-frequency measurements using Acoustic Doppler Velocimetry (ADV) were carried out on a 1:10 scaled experimental setup with a fixed model dune in a closed-circuit flume. Results show that over the steep portion of the dune lee side, a flow separation zone with a recirculating flow cell and a turbulent wake develop. Compared to values reported for triangular and river dunes, a longer flow separation zone (6.5 times the height of steep portion) and a downward oriented, shorter wake (5.5 times the height of the steep portion) were found. The high-quality experimental dataset including the flow velocity timeseries is freely available at https://doi.org/10.48437/02.2021.K.9900.0001 (Bundesanstalt für Wasserbau 2021) and can be used for further studies, e.g. on the dissipative effect of dunes, or as validation data for laboratory experiments and mathematical models. Overall, we give indication for the need to study hydrodynamic processes related to estuarine dunes in more detail and we provide a full description of the experimental setup and the complete collected dataset to support and facilitate the needed further research.

## Keywords

estuarine dune, flume experiments, ADV, turbulent kinetic energy, validation data

## Zusammenfassung

*In Ästuaren und Küstenbereichen sind Bodenformen wie Dünen weit verbreitet. Dünen verursachen einen Fließwiderstand, infolgedessen Energie dissipiert wird. Auf diese Weise beeinflussen Dünen die hydrodynamischen Prozesse wie auch den Sedimenttransport im Gewässer. Die Prozesse bei der Überströmung sind komplex und variieren in Abhängigkeit der Dünenmorphologie. Insbesondere Dünenformen, wie sie in Ästuaren auftreten, wurden bisher kaum betrachtet, obwohl für großräumige Untersuchungen von Ästuaren mit numerischen Modellen eine genaue Kenntnis der hydrodynamischen Vorgänge wichtig ist. Um diese*


Received 15. August 2023, Reviewed 09. October 2023, Revised 23. November 2023, Accepted 11. January 2024, Available online 25. January 2024

*Lücke zu schließen, wurden erstmalig physikalische Modellversuche mit einer ästuarinen Düne durchgeführt. Der Versuchsaufbau ermöglichte die großmaßstäbliche Untersuchung der Strömungsprozesse über der Düne in einem hohen Detailgrad. Hochfrequente Strömungsmessungen mit ADV (Acoustic Doppler Velocimetry) wurden an einem 1:10 skalierten Versuchsaufbau mit einem fixierten Dünenmodell durchgeführt. Die Ergebnisse zeigen, dass über dem steileren Abschnitt der Dünenleeseite eine Strömungsablösung mit einem Strömungswirbel sowie eine turbulente Nachlaufströmung auftreten. Im Vergleich zu dreieckförmigen Dünen und Flussdünen wurden ein längerer Strömungswirbel (6,5-fache Höhe des steilen Böschungsabschnitts) und eine nach unten gerichtete, kürzere turbulente Nachlaufströmung beobachtet (5,5-fache Höhe des steilen Böschungsabschnitts). Der umfangreiche Datensatz mit den gemessenen Zeitreihen der Strömungsgeschwindigkeiten ist frei verfügbar unter https://doi.org/10.48437/02.2021.K.9900.0001 (Bundesanstalt für Wasserbau 2021) und kann für weitere Studien z. B. zur Rauheitswirkung von Dünen oder zur Validierung physikalischer oder numerischer Modelle verwendet werden. Insgesamt zeigen wir auf, dass hydrodynamische Prozesse über ästuarinen Dünen zukünftig detailliert untersucht werden sollten und liefern hierfür als Grundlage eine ausführliche Beschreibung des Versuchsaufbaus und den vollständigen experimentellen Datensatz, um die erforderliche weitere Forschung zu unterstützen.*

## Schlagwörter

*Ästuarine Düne, Rinnenversuche, ADV, Turbulente kinetische Energie, Validierungsdaten*

## 1 Introduction

Bedforms are observed over wide areas in natural free-flowing waters like rivers and estuaries. They are found in various geometries and sizes and are often classified as ripples or dunes. Ripples are small-scale bedforms with lengths of less than 0.6 m, while dunes are large-scale bedforms with lengths of more than 0.6 m up to more than 100 m (e.g. Ashley 1990). Whereas the height of current ripples is independent of the water depth and described as less than 0.03 m, the height of dunes is reported to scale with water depth (Bennett and Best 1995, Venditti 2013). Bedform existence, size and shape depend on flow and sedimentary conditions. At the same time, bedforms influence the flow by acting as roughness elements that dissipate flow energy not only by friction of the single sediment grain but also by form friction when the water flows over the bedform. This means that there is a complex interaction between bedforms, hydrodynamic processes and sediment transport.

For estuarine and coastal processes, especially dunes are relevant due to their size and related form friction (e.g. Dalrymple and Rhodes 1995, Winter et al. 2016, Lefebvre et al. 2021). However, a precise and quantitative knowledge of their dissipative effect is still not available, although this is an important aspect e.g. for a correct parameterization in mathematical hydrodynamic models (Herrling et al. 2021). The difficulty to precisely describe the dissipative form friction effect is caused by the complex small-scale hydrodynamics of the overlying flow that varies depending on the geometry of the dune and especially of the dune lee side.

At dunes with lee sides with an angle-of-repose (~ 30°), a flow separation zone with a recirculating flow and a turbulent wake develops, leading to enhanced dissipation of flow energy (e.g. Best 2005, Venditti 2013). These processes are in particular observed over two-dimensional dunes with a steep-slope angle and a triangular shape, as they occur in small rivers or in laboratory flumes with unidirectional currents.

In larger rivers, dunes often have slopes with angles smaller than angle-of-repose (Kostaschuk and Villard 1996, Cisneros et al. 2020). Unlike angle-of-repose dunes, flow separation and recirculation over low-angle dunes is absent or intermittent, as previous research showed. Based on numerical simulations, Lefebvre and Winter (2016) suggested that below a lee side angle between 11° and 18° no flow separation and reverse flow are present. Laboratory experiments conducted by Best and Kostaschuk (2002) demonstrated, that on lee side angles of 14° the flow recirculation is intermittent. Laboratory dunes studied by Kwoll et al. (2016) showed intermittent flow recirculation at lee side angles of 10° and 20°.

Furthermore, natural dunes usually have an asymmetrical shape, variations in curvature and low angle slopes often composed of brink points and portions with different angles (Kostaschuk and Villard 1996, Parsons et al. 2005, Lefebvre et al. 2016). For complex dune geometries, it was found that the steepest part of the lee side controls the occurrence of flow separation (Lefebvre et al. 2016). Lefebvre (2019) suggested that flow separation and increased turbulence are present for slope portions steeper than 15°.

For river dunes, the steepest part of the dune slope was found to be in the lower half of the lee side close to the trough (Lefebvre et al. 2016, Cisneros et al. 2020). On the contrary, for estuarine dunes the steepest part is reported near the crest in the upper half of the slope (Dalrymple and Rhodes 1995, Lefebvre et al. 2021). Until now, experimental and numerical studies have mainly focused on bedforms of simple geometry and only few studies have been conducted on investigating flow characteristics over dunes with segmented lee sides (Paarlberg et al. 2007, Kwoll et al. 2016, Lefebvre et al. 2016). These dunes, however, resembled river dunes with the steepest part near the trough. To our knowledge, flow properties over dunes with a steep portion near the crest, thus resembling estuarine dunes, have not been extensively studied so far.

Laboratory methods allow for detailed measurements of flow and turbulence characteristics over dunes in a controlled parameter space. In the past, detailed measurements were limited, e.g. due to difficulties performing near-bottom measurements in the field (Best and Kostaschuk 2002, Kostaschuk and Best 2005, Parsons et al. 2005) or due to the dimensions of the facility and thus small-scale experiments with dune heights in the range of 2–3 cm (Nelson et al. 1993, Best and Kostaschuk 2002, Kwoll et al. 2016). As these aspects may limit the identification of flow separation at the dune lee side, the aim of our study is to investigate the flow properties over a typical estuarine dune on a large scale and to build a setup with the capability of studying dunes based on detailed measurements.

Here, we study flow over a single, large-scale two-dimensional estuarine model dune in a laboratory flume to estimate the occurrence and size of the flow separation zone and the turbulent wake. The dune is shaped with a steep portion near the dune crest on the lee side with an angle of more than 15°, here referred to as the “steep face”. To isolate the effect of the dune shape and the steep face angle on the flow structure, experiments were carried out with a fixed model dune and constant hydraulic parameters (i.e. unidirectional flow, constant flow velocity and water level). High-frequency measurements were conducted to characterise the flow field and the turbulent kinetic energy (TKE).

# 2 Methods

## 2.1 Flume Setup

Experiments were conducted in the 1.5 m wide closed-circuit flume at the Federal Waterways Engineering and Research Institute (BAW) in Hamburg. The flume has two straight sections connected at their respective ends by semi-circular sections forming a closed-circuit flume with a total length of 220 m. The rectangular test section is about 70 m long and 1.5 m wide. The flow is generated by a bow thruster located in an underground pipeline on the opposite side of the test section. A photograph and a schematic drawing of the closed-circuit flume are shown in Figure 1.

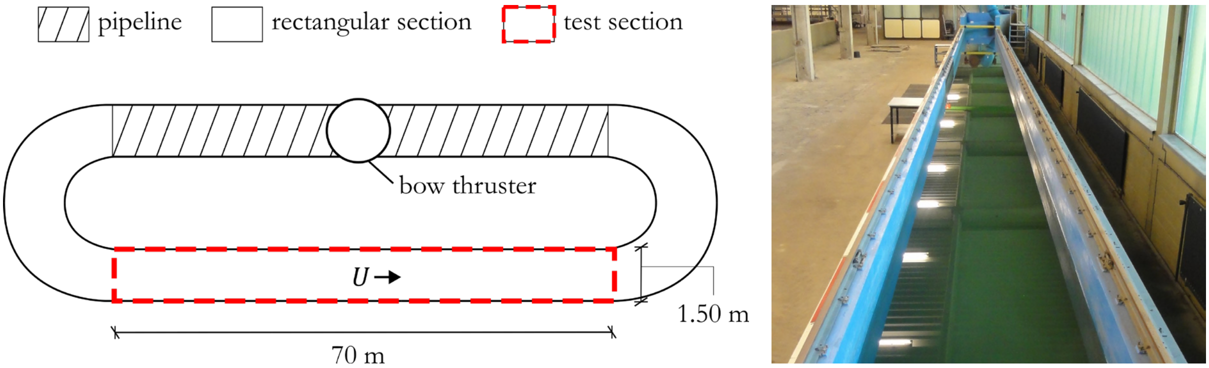


Figure 1: 1.5 m wide closed-circuit flume: Schematic drawing (not to scale, left) and photograph of the test section (right).

Prior to the dune experiments, detailed investigations were carried out on the occurrence of secondary flows in the test section. These secondary flows can be induced, for example, by the geometry of the inlet area, or by the propeller motion of the bow thruster. Measurements showed that in the rear part of the flume influences of a secondary flow are neglectable and the flow is only controlled by local boundary conditions. Therefore, the experiments were carried out in the flume's rear section at a distance of about 50 m from the inlet area (see also Figure 3).

## 2.2 Dune Design and Hydrodynamic Conditions

The model dune dimensions and shape were based on results of an investigation of the dune morphology and characteristics in the Weser Estuary by Lefebvre et al. (2020). Asymmetrical, ebb-oriented dunes with a steeper portion on the lee side (ebb steep face) were frequently found, so this dune type was used as a prototype for the scaled model dune. Heights $H$ of the ebb-oriented dune in the Weser River were found in a range of 1.2 m to 1.8 m, lengths $L$ from about 30 m up to 60 m, mean slope angles of 5° to 8° on the steeper lee side and 2° to 5° on the lower stoss side. The range of dimensions and slope angles of the ebb-oriented dune with an ebb steep face in the field are summarized in Table 1, a schematic drawing is given in Figure 2.

Table 1: Representative dimensions and slope angles of the ebb-oriented dune with an ebb steep face from Weser Estuary, according to Lefebvre et al. (2020).

| | |
|---|---|
| Length $L$ | 30 - 60 m |
| Height $H$ | 1.2 – 1.8 m |
| Aspect Ratio $H/L$ | 0.02 – 0.05 |
| Mean lee side angle | 5° – 8° |
| Mean stoss side angle | 2° – 5° |

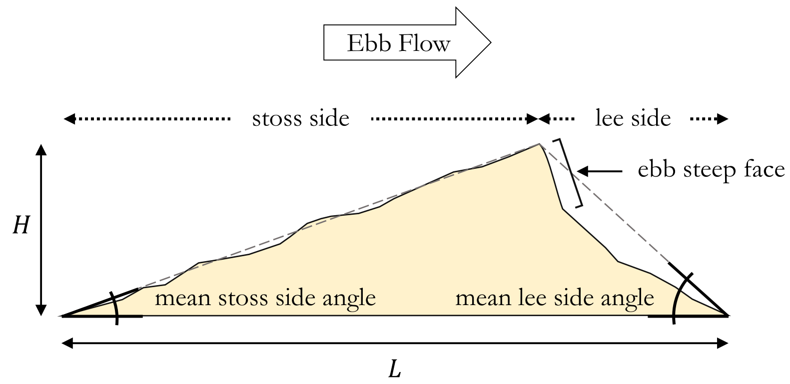


Figure 2: Schematic drawing of an ebb-oriented dune with an ebb steep face.

The dimensions of the model dune were selected from this range of values and are considered representative of the observed dune type. The model dune was scaled by a factor $N_L$ of 10 according to Froude's Law (Table 2). It was built asymmetrical with a length of 3 m and a height of 0.15 m. The stoss side angle was 4°. The leeward side consisted of two portions, a steep face of 25° and 0.24 m length starting at the crest and a lower and longer portion (4° and 0.80 m length) towards the trough. The height of the steep face $H_{SF}$ was 0.10 m. Compared to naturally occurring ebb-oriented dunes in the Weser river, a relatively steep and long steep face was chosen in order to produce a fully developed, permanent flow separation which forms at slope angles steeper than 24° (Lefebvre and Winter 2016). A schematic drawing of the model dune is shown in Figure 3. The model dune was made from a thick metal sheet, which was bent into shape (Figure 3, right) and attached to the flume bottom.

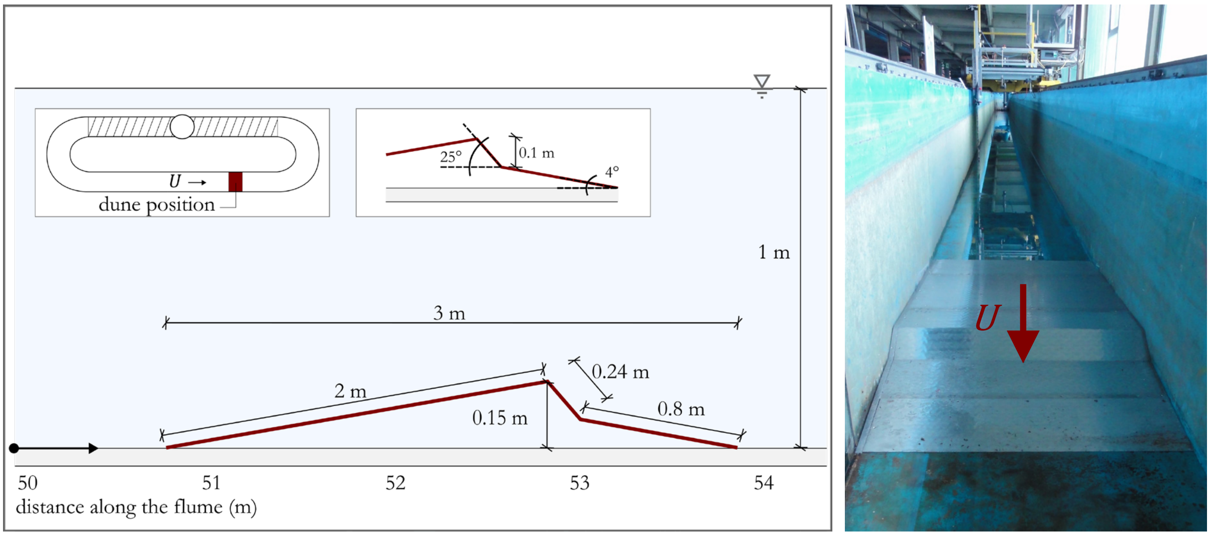


Figure 3: Schematic drawing of the model dune dimensions (not to scale) and position in the flume (left) and view of the model dune in the flume (right).

For the hydrodynamic model parameters, water level data of a local measuring station in combination with a digital terrain model (DTM) from 2012 were used (WSV 2020, inphoris GmbH and smile consult GmbH 2014). For the assessment of realistic flow velocities, data from flow measurements using an Acoustic Doppler Current Profiler (ADCP) from 2009 to 2011 (Bundesanstalt für Wasserbau 2016) were considered. The measurements were taken in the area of Weser-km 47 (Rechtenfleth), where ebb-oriented dunes with an ebb steep face are found according to Lefebvre et al. (2020). Influenced by tides, flow direction and flow velocities in the Weser Estuary change from one tidal phase to the next. For the experiments, these dynamics were not represented and a steady, unidirectional flow was considered for simplification. In the area in which ebb-oriented dunes with an ebb steep face were found, maximum flow velocities during ebb were about 0.9 m/s to 1 m/s (Bundesanstalt für Wasserbau 2016), the mean flow depth was about 14 m.

It was not intended to represent field hydrodynamics exactly, but to find realistic parameters that represent a typical order of magnitude of the field values. Thus, a constant depth-averaged flow velocity $U$ of 0.3 m/s in model scale representing velocities of approximately 1 m/s during the ebb phase was chosen for the experiments. The observed average flow depth of 14 m in the field corresponds to a water depth of 1.4 m in model scale, which cannot be realised in the laboratory flume (maximum filling level: 1.3 m). However, preparatory tests showed that the relevant flow processes over the dune in the flume setup take place within a water depth of less than 1 m and are not influenced by slight changes in water level. Thus, a water depth $d$ of 1 m at model scale was selected for the laboratory tests (corresponding to a field water depth of 10 m). The considered field dimensions and hydrodynamic parameters as well as the representative model parameters in 1:10 scale are summarised in Table 2.

Table 2: Flow and dune characteristics in field and model scale

| Scale $N_L$ = 10 | Scale Factor | Field | Model |
|---|---|---|---|
| Length $L$ | $N_L$ | 30 m | 3.0 m |
| Height $H$ | $N_L$ | 1.50 m | 0.15 m |
| Height of steep face $H_{SF}$ | $N_L$ | 1 m | 0.10 m |
| Aspect ratio $H/L$ | - | 0.05 | |
| Average lee side angle | - | 8° | |
| Stoss side angle | - | 4° | |
| Steep face angle | - | 25° | |
| Water depth $d$ | $N_L$ | 10 m | 1 m |
| Depth-averaged flow velocity $U$ | $\sqrt{N_L}$ | 1 m/s | 0.3 m/s |
| Froude Number | - | 0.1 | 0.1 |
| Reynolds Number | - | - | $3 \cdot 10^4$ |

## 2.3 Data Collection

Measurements were carried out with a Nortek Vectrino (ADV). The instrument used was a down-looking type, where the emitter and receiver arms are oriented downwards. Thus, the sampling volume is located below the probe head and measurements can be taken close to the dune slopes and the flume bottom.

A total of approximately 1600 measurements of flow velocity time series were collected over the model dune in each of two test repetitions, distributed across 46 length positions along the centre axis of the flume (Figure 4). Over the stoss side, the horizontal distance between two sampling locations was 20 cm and the vertical distance was 2–3 cm. For a sufficient detection of the turbulent flow at the dune lee side, the horizontal distance was reduced to 10 cm near the dune crest and to 5 cm behind the crest. In the lower part of the water column near the slopes, the vertical distance was condensed to 1 cm. In the area behind the dune, the horizontal distance was again increased to 10 cm. A motor-controlled motion unit ensured a precise positioning of the instrument. The reproducibility of the recorded data was verified by a first measurement and a repeat measurement at each sampling position.

Velocity time series were recorded at a high-frequency sampling rate $SR$ of 100 Hz for 4 min in the turbulent areas near the slopes at the dune lee side and for 2 min at the remaining positions. For each sampling position, the instantaneous velocities in the direction of flow, in the cross-stream direction and in the vertical direction, $u_i$, $v_i$ and $w_i$, respectively, were recorded over the selected measurement duration. Index $i$ indicates the sample at the time $1/SR \cdot i$.

The instrument was collecting flow velocity components in a cylindrical sampling volume of 4 mm height and 6 mm diameter. The blanking distance between the probe head and the sampling volume was generally set to 5 cm, as this is referred to as the sweet spot of the instrument, where best quality data can be measured (Nortek 2018). Only in few cases a different blanking distance was used when the measurement positions could only be reached by adjusting this value (e.g. near the water surface).

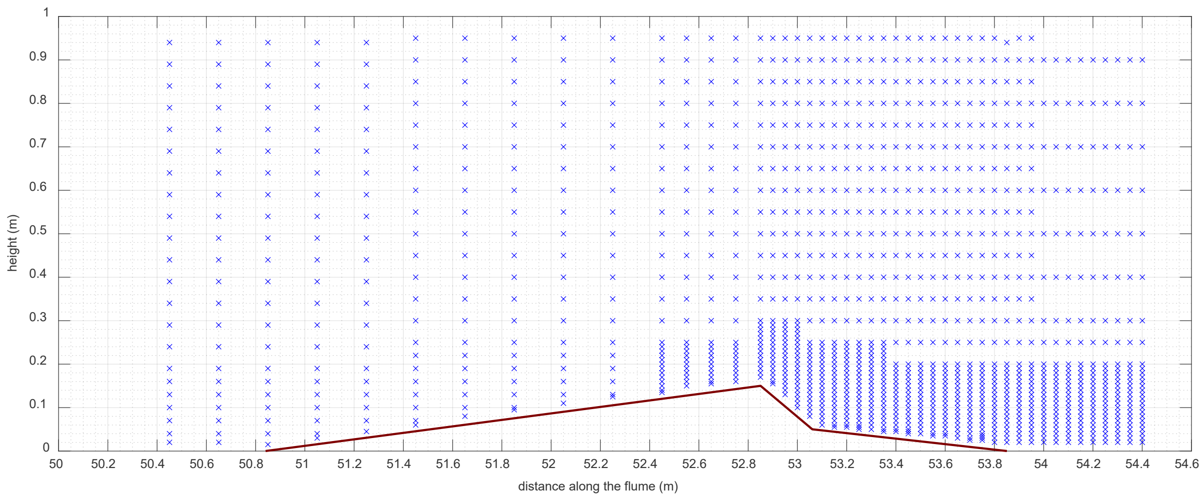


Figure 4: Sampling positions for flow velocity measurements over the model dune.

The probe's settings were chosen in order to achieve the highest possible data quality. A good data quality was assessed especially on the basis of the values for signal-to-noise ratio (SNR) and correlation. Overall, the experimental conditions required only minor adjustments to the once selected configurations, as the SNR values recommended for reliable data acquisition in the range of about 30 dB and a correlation above 90 % could be attained. Because of the naturally occurring suspended sediment in the water used for the experiments, no additional seeding material had to be added to ensure sufficient reflections of the acoustic signal of the ADV.

The measurements were processed by converting the raw data into a Matlab-file and using custom codes for import and error filtering, which included despiking the data, i.e. the identification and removal of outliers in the velocity time series. Several approaches are available for despiking ADV data, of which the Phase-Space Thresholding Method after Goring and Nikora (2002) was used. An additional filtering of the data according to SNR and correlation threshold values was not performed, since by applying the Phase-Space Thresholding Method data with low correlation and SNR were already removed from the timeseries.

# 3 Mean and Turbulent Flow Field

## 3.1 Flow Field

The extensive measurements allowed a detailed characterisation of the mean flow field above the dune. The magnitude of the flow velocity and the flow direction over the dune were analysed in order to investigate the flow separation and recirculation. After processing and error filtering the collected data, mean flow velocities were calculated for each velocity component time series as

$$\bar{u} = \frac{1}{N}\sum_{i=1}^{N} u_i \tag{1}$$

and $\bar{v}$, $\bar{w}$ accordingly, where $\bar{u}$, $\bar{v}$, $\bar{w}$ are the time-averaged streamwise, crosswise, vertical velocity components, respectively, and $N$ is the total number of measurements at each location. Since a two-dimensional dune was investigated, the overlying flow field was also analysed two-dimensionally. Velocity vectors $(\bar{u}, \bar{w})^T$, considering the mean of the horizontal, streamwise velocity component in flow direction $\bar{u}$ and the mean of the vertical velocity component $\bar{w}$, are presented in the following figures of this section. The mean of the horizontal, crosswise velocity component $\bar{v}$ is not included in these two-dimensional visualisations of the flow field. The mean value of $\bar{v}$ of all measurements is 0.0092 m/s. Accordingly, either a small crosswise flow velocity component existed or the ADV probe was not perfectly aligned with the main flow direction. Since $\bar{v}$ is only 3 % of the depth-averaged flow velocity ($U$ = 0.3 m/s) and therefore hardly deviates from the expected value of $\bar{v} = 0$ m/s for an ideal two-dimensional flow, $\bar{v}$ can be neglected here.

Regarding the repeatability of the measurements, a very good agreement could be obtained for the recorded flow velocities from the first and the repeat measurement. A high level of agreement for the flow velocity vectors, i.e. corresponding in magnitude and direction, between the first and the repeat measurement are found throughout the recorded flow field. In particular, a very good agreement can be observed in the area of the dune lee (Figure 5), which is the crucial part of the flow processes. Overall, 93 % of the magnitude deviations of the calculated velocity vectors are less than 0.015 m/s, which corresponds to less than 5 % of the generated depth-averaged flow velocity of $U$ = 0.3 m/s. Only in 12 out of a total of 3312 measurements, magnitude deviations of more than 0.03 m/s (10 % of $U$) were detected.

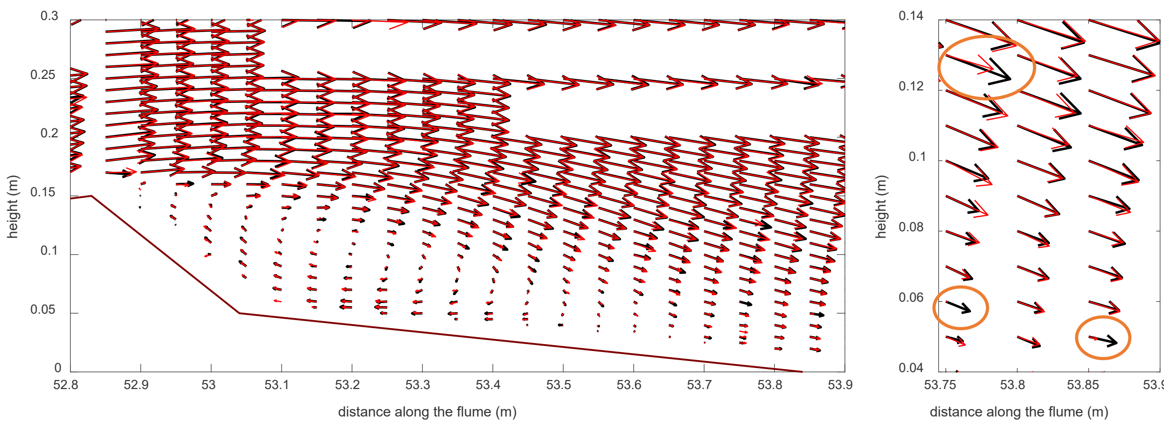


Figure 5: Measurement's repeatability: Flow velocity vectors $(\bar{u}, \bar{w})^T$ of first (black) and repeat measurement (red). Overall good repeatability at dune's lee (left figure), outliers at the rear of the slope (right figure).

Of these, 3 measurements can be identified as outliers with deviations between 0.06 m/s and 0.08 m/s at distances of 53.75 m and 53.85 m along the flume (Figure 5, right). At these length positions, a lower SNR performance was found for the bottom measurement positions. For measurements of good data quality, SNR values were observed in a constant value range along the entire vertical profile. However, at length positions 53.75 m and 53.85 m, the average SNR value for the bottom measurement positions containing the outliers (up to 0.15 m above ground) was about 5 dB lower than the average SNR value for measurements in the upper part of the water column. This is probably related to interferences with the nearby bed surface (i.e. the dune slope), described as weak spots of the instrument. At weak spots, the measurement principle of the ADV probe is disturbed and the data quality reduced, leading to measurement inaccuracies (Nortek 2018). Nevertheless, a good repeatability of the measurement and therefore reproducible data was observed because of the low number of outliers. Thus, only the first repetition of the measurements is referred to in the following analysis.

Figure 6 shows the velocity vectors $(\bar{u}, \bar{w})^T$ over the entire model dune. The flow velocity magnitude is colour coded and also qualitatively represented by the length of the vectors. The distribution of the mean flow velocities over depth follows a logarithmic profile in vertical direction which is typical for turbulent flows. Due to boundary layer friction, velocities decrease towards the bottom. The highest velocities are found in a height of 0.55 m to 0.80 m above ground with values of 0.36 m/s to 0.41 m/s.

Topographic forcing causes flow acceleration above the stoss side and flow deceleration above the lee side of the dune. As shown enlarged in Figure 7, a flow separation zone can be detected in the dune lee with a recirculating flow cell. The flow separation zone begins shortly behind the dune crest and extends downstream. The reattachment point to the undisturbed flow is located shortly before the model dune slope ends. The length of the flow separation zone $L_{FSZ}$, which is defined by horizonal length of the area where a backward flow could be detected, is approximately 0.65 m in model scale (cf. Figure 7), corresponding to $4.3 \cdot H$ and $6.5 \cdot H_{SF}$.

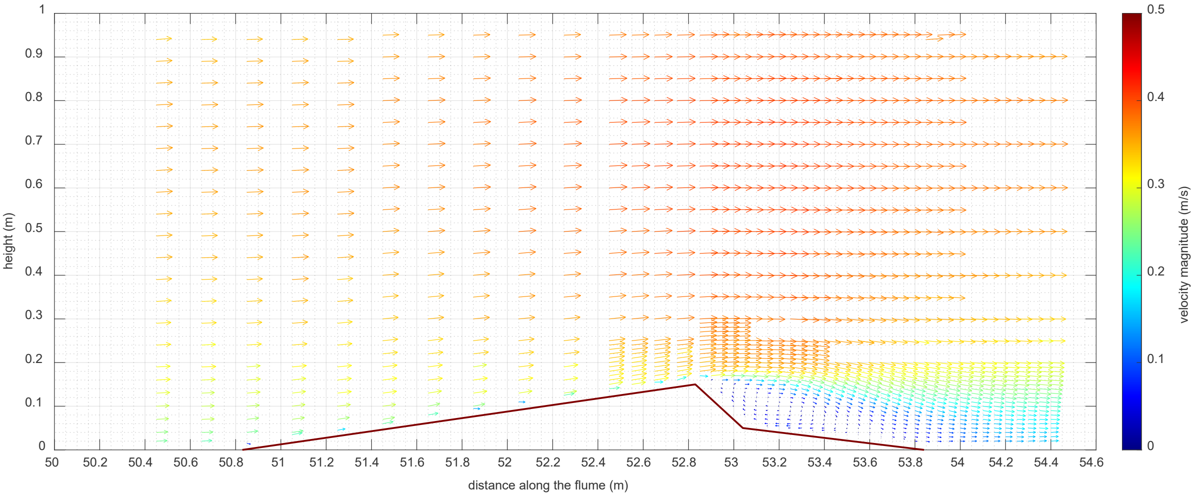


Figure 6: Mean flow velocity vectors $(\bar{u}, \bar{w})^T$ above the model dune.

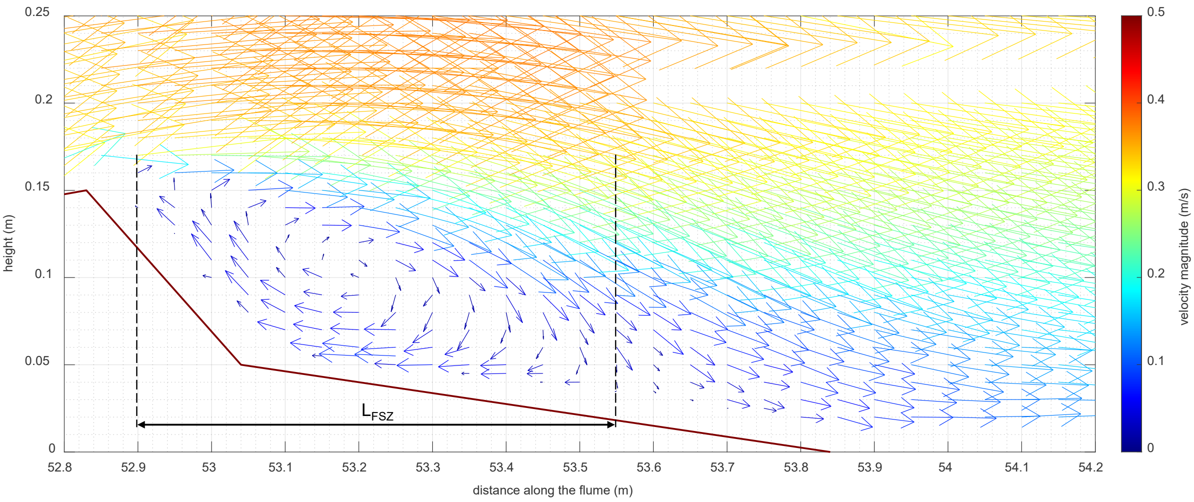


Figure 7: Flow separation zone with recirculating flow cell at the dune lee side.

## 3.2 Turbulent Kinetic Energy

The turbulent kinetic energy (TKE) was calculated from the collected data in order to identify the turbulent wake and estimate the turbulence intensity over the dune. The TKE contained in the turbulent eddies of the flow was determined from the variances of the measured velocity components as

$$TKE = ½ \cdot \left(\overline{u'u'} + \overline{v'v'} + \overline{w'w'}\right), \tag{2}$$

where

$$\overline{u'u'} = \frac{1}{N}\sum_{i=1}^{N}(u_i')^2 = \frac{1}{N}\sum_{i=1}^{N}(u_i - \bar{u})^2, \tag{3}$$

and $\overline{v'v'}$, $\overline{w'w'}$ accordingly. $u'$, $v'$ and $w'$ are the streamwise, crosswise and vertical fluctuations around the mean value of the velocity components, where

$$u_i' = u_i - \bar{u}, \tag{4}$$

and $v_i'$, $w_i'$ accordingly.

As Figure 8 shows, higher TKE values can be observed in the dune lee, forming a turbulent wake. The zone with higher TKE values begins shortly behind the dune crest and extends downstream along the lee slope in a downward direction. TKE is highest in the middle of the wake zone above the lower, gentle sloping part of the leeside ($TKE_{\max}$ = 0.01 m²/s², Figure 9).

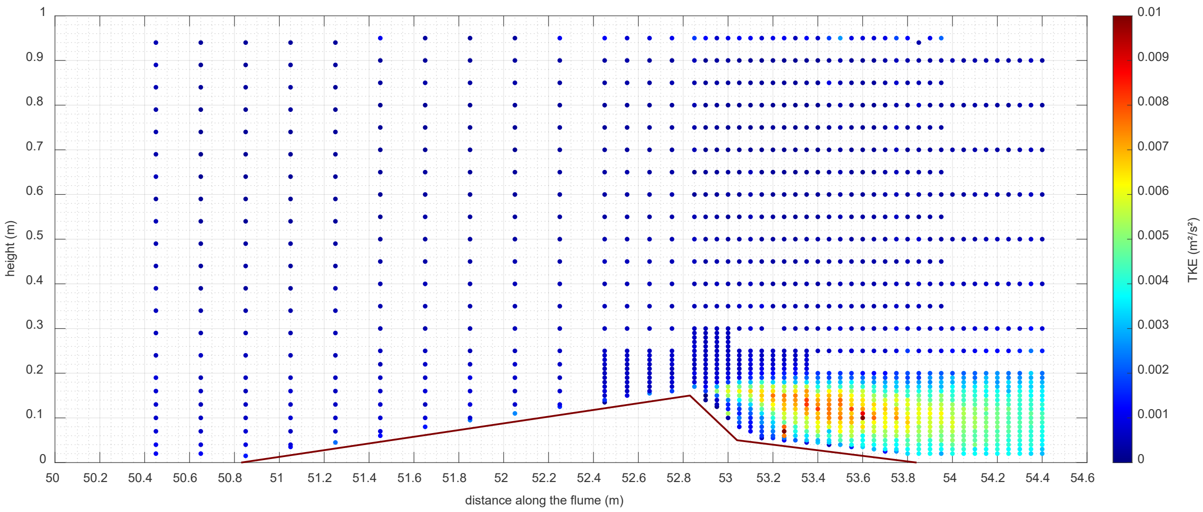


Figure 8: Overview of TKE values and their distribution over the model dune.

Outside the turbulent wake, few positions near the dune slope were found to also have a higher TKE (cf. Figure 9, at distance along the flume of 53.25 m). Analyses of the measured time series at these locations revealed that correlation values and SNR of the data were comparably low and increased, respectively. This indicates disturbances during data recording, likely due to increased return signal levels from reflections at the nearby dune surface impairing the ADV measurement method and data quality. Thus, these data points are to be interpreted as outliers due to sampling inaccuracies.

Defining the turbulent wake by the area in which the TKE is at least 70 % of the maximum measured TKE value ($TKE_{70}$) and excluding the outliers, the horizontal length of the turbulent wake $L_W$ is 0.55 m (cf. Figure 9). This length definition of the turbulent wake will be discussed in Section 4.

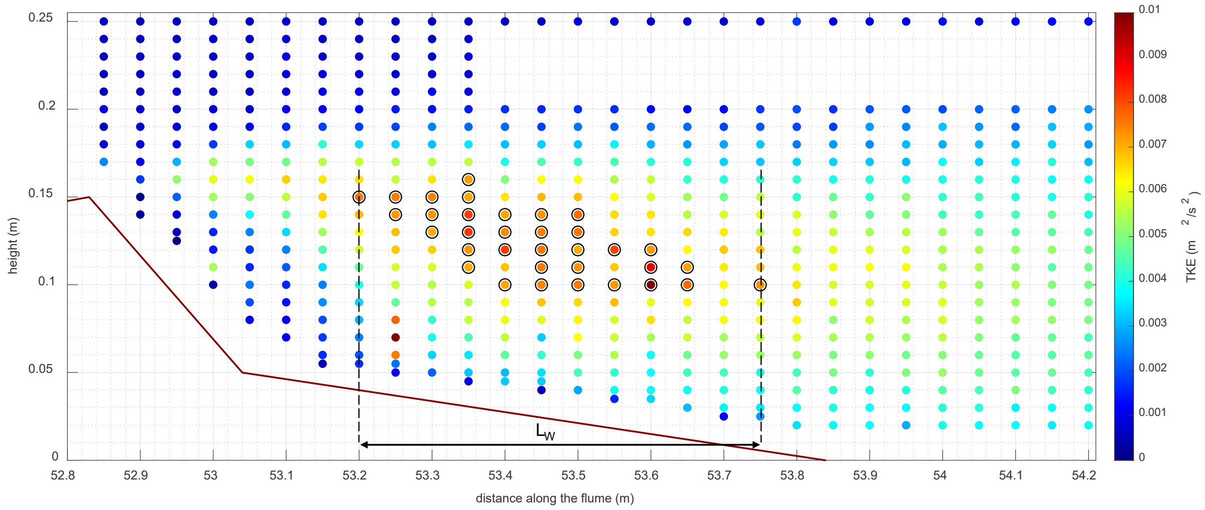


Figure 9: Turbulent wake over the dune lee, 70 % highest TKE values marked (without outliers).

# 4 Discussion

## 4.1 Model settings

The large-scale experimental setup allowed for measurements over the model dune with closely distributed sampling positions. By using a fixed model dune, measurements could be carried out over a long period of time and at many different measuring positions without changing the shape and position of the dune. Since a constant flow velocity and water level were set based on the maximum ebb current velocity and a water level found in the Weser River, the experiments were performed under controllable, realistic hydrodynamic conditions. From various dune lengths, heights, slope angles, steep face characteristics and shapes occurring in natural estuaries, typical dimensions and a frequently found dune shape from the Weser River were chosen here to exemplify the range of different morphologies.

While sediment transport and the effect of dune migration or reshaping under full tidal dynamics were not investigated in this experiment, the flow field above the estuarine-type dune could be represented in an unprecedented large-scale setup. Due to the large model dimensions, measurements could be carried out at 46 horizontal positions covering an approximately 4 m long section above the dune with a varying resolution that was highest in the lee of the dune with a vertical resolution of 1 cm. In the past, laboratory measurements at a similar level of detail have been conducted over dunes on a much smaller scale. Best and Kostaschuk (2002) performed measurements with a high vertical resolution of 1–2 mm over a fixed low-angle dune. However, the model dune was scaled 1:58, corresponding to a model height of 3.1 cm and model length of 66 cm. Measurements by Kwoll et al. (2016) over a segmented model dune were also closely distributed with a vertical and horizontal resolution of 5 mm near the dune slope and 10 mm outside the lee region, respectively, but again the dune was only 3 cm high and 90 cm long. Kwoll et al. (2016) noted that regions of weaker flow separation decrease in size with lower lee angle and therefore, the detection of flow separation strongly depends on where the observations were made. The large scale of the dune used here is therefore an advantage regarding the positioning accuracy and, in combination with the high number and high spatial resolution of the measurement positions, is thus beneficial for the identification of flow separation over the dune lee side.

## 4.2 Flow separation zone

In accordance with observations from previous studies on dunes, behind the model dune steep face of 25° (which exceeds the thresholds range for flow separation of 10°–20° mentioned in the literature, cf. Section 1) a flow separation with a flow recirculation cell is present and a turbulent wake develops. For triangular dunes with a simple lee slope, the length of the flow separation zone is often cited as 4–6 times the dune height (Engel 1981, Fernandez et al. 2006). Studies of dunes with segmented lee sides and lee sides containing a steeper portion showed that the length of the flow separation zone is especially related to the properties of the steep face (Lefebvre et al. 2016, Lefebvre 2019). For dunes with a steep face near the dune trough, as typical of river dunes, it was found that the length of the flow separation zone is about 4–6 times (Paarlberg 2007), 5 times (Lefebvre 2019) the height of the steepest part of the slope or even smaller with 3.6 times the steep face height (Lefebvre et al. 2016). For the estuarine model dune investigated here, the length of the flow separation zone $L_{FSZ}$ is about 0.65 m, which corresponds to $6.5 \cdot H_{SF}$ and is thus longer than the values given in the literature. The reason for this is that the flow separation at the estuarine dune shape begins at the dune crest where the steep face is located, and thus appears to expand over a greater distance further downstream along the gently sloping lower lee side. In contrast, at dunes with their steep face located near the trough, as typical for river dunes, the rising slope of the next dune is directly neighbouring the flow separation zone and leads to a shortening of the flow recirculation cell.

## 4.3 Turbulent wake

The turbulent wake over the model dune, which is characterised by a zone with higher TKE, originates at the dune crest and extends downstream in a slightly downward direction. Compared to observations from other studies, this is different from a wake over a triangular bedform, where the wake appears to expand upwards (cf. Fernandez et al. 2006, Lefebvre et al. 2014b) as it is pushed up by the topographic forcing of the following dune stoss side. The maximum TKE values measured over the model dune are about 0.008 $m^2/s^2$ to 0.01 $m^2/s^2$ and are comparable to values in the literature: For example, experiments on laboratory dunes by Kwoll et al. (2016) carried out with a higher mean flow velocity of 0.62 m/s and at a shallower water depth of 0.2 m and thus a higher Reynolds number of $1.24 \cdot 10^5$, showed a maximum TKE value of 0.011 $m^2/s^2$ over a dune with the same relative height ($H/d = 0.15$) and a 20° lee side angle. This value is slightly higher than for the present results, but corresponds to the order of magnitude of the values found in this study.

Regarding the length of the turbulent wake, different definitions are found in the literature. In Lefebvre et al. (2014a) and Lefebvre et al. (2014b), the wake length is defined as the horizontal length of the area in which the TKE is at least 70 % of the maximum measured TKE value ($TKE_{70}$). Lefebvre (2019) proposed a different definition for the wake length, which is the horizontal length of the area where the TKE is larger than the TKE 98$^{th}$ percentile ($TKE_{98}$). However, this publication also highlights that a standard definition of the turbulent wake over bedforms is still not agreed on. For our measurements, both the calculations according to $TKE_{70}$ and $TKE_{98}$ result in a length of the turbulent wake $L_W$ of 0.55 m. In Figure 9 in Section 3, we illustrated $TKE_{70}$ because this measure is simple to apply and delivers valid results also for small datasets (as long as the wake and the maximum TKE are sufficiently captured).

The length of the turbulent wake over the estuarine dune found in this study corresponds to 5.5 times the height of the steep face ($L_W = 5.5 \cdot H_{SF}$). For numerically modelled 3D river dunes with a steep face, Lefebvre (2019) proposed the relation between the steep face height and the wake length to be $L_W = 13 \cdot H_{SF}$. Thus, the relation found from our experiments indicates shorter wake lengths occurring over an estuarine dune. However, in a prior study on angle-of-repose dunes of Lefebvre et al. (2014b), shorter turbulent wake lengths in the laboratory compared to numerical experiments were also found. There, it was assumed that the wake was shortened due to friction from the laboratory flume walls, while full slip conditions were used in the numerical model. Therefore, also in our study wall friction might be one of the reasons for the smaller wake length found in comparison to results from numerical simulation of Lefebvre (2019).

Nevertheless, due to the large extend of the flow separation cell and the downward extending wake observed here behind the estuarine dune shape, a greater potential for the mobilization of bottom sediments compared to triangular dune and river dune shapes, where an upward extending wake develops, might be possible.

## 4.4 Limitations

However, some limitations to these findings are given due to the simplifications that were made with regard to the dune design and the modelled, hydrodynamic conditions. One simplification of this setup is that only a single bedform was installed in the flume. Thus, the model dune slope at the lee side is followed by the horizontal flume bottom. The neighbouring shapes of leading and following dunes are likely to influence the flow structure. This may have an effect on the length of the flow separation zone as well as on the downward or upward orientation of the wake. However, for the recirculating flow observed here, this is not necessarily to be expected, since the observed recirculation cell does not extend over the entire lower lee side and ends before a next dune stoss side would begin. Another simplification is the two-dimensional dune design with straight slopes and without superimposed ripples, as found in the field. Since the dune was made of metal plates without a sand coating, the natural surface roughness of dunes in the field was also not reproduced. The flow and turbulence processes identified in the experiment therefore are a simplified representation of the natural processes occurring over a dune field in estuaries and, due to the missing grain and ripple roughness, energy dissipation might be underestimated. Nevertheless, the dataset is a consistent report of the effect of a so far uninvestigated bedform shape to unidirectional flow, ready for use in evaluation studies of numerical models.

# 5 Data Availability

The consistent and comprehensive dataset of the flow measurements over the model dune is available for download at https://doi.org/10.48437/02.2021.K.9900.0001 (Bundesanstalt für Wasserbau 2021). The provided dataset contains the raw data from the first and repeat measurement for each sampling position. In addition to the flow velocities time series in all three spatial directions, the files contain all recorded, probe-specific parameters including SNR and correlation values as important parameters for assessing the data quality.

## 6 Conclusions

A laboratory setup to study flow over a single model dune in a closed-circuit flume was designed, built and successfully operated. Flow velocity data, sampled at high-frequency with an ADV, were obtained by closely distributed measurement positions even close to the dune slopes and bottom on an unprecedented large-scale model. In contrast to other studies, the investigated model dune resembled a shape typical for estuarine dunes with a steep slope face in the upper half of the lee side near the dune crest.

Results give indication that different hydrodynamic characteristics are observed over estuarine dunes in comparison to river or triangular dunes. In particular, a greater length of the flow separation zone and a downward orientation of the turbulent wake are identified. Here, further research is needed to confirm the observed characteristics and to consider the possible influence of different forcing conditions, estuarine dune shapes, neighbouring dunes and a realistic surface roughness.

Nevertheless, the scale of the experimental setup proved suitable for the generation of high-quality data that allow a detailed assessment of the flow processes and the distribution of turbulence intensity over a model dune.

The extensive dataset is provided with full accessibility, in order to provide an opportunity to validate experimental and numerical models. Furthermore, the data can be used as reference data for further studies and analyses of flow over dunes. Therefore, the here presented work is a profound basis for ongoing experimental and numerical work to build up a quantitative knowledge about the dissipative effect of estuarine dunes.

## 7 Acknowledgements

We thank: Frank Kösters, who initiated the project; the BAW Hamburg laboratory team and especially Bernhard Kondziella and Lars Tretau for providing technical support during the experimental setup and procedure; Katja Schulz for her contributions to the extensive flow measurements. This work was funded as part of the Federal Waterways Engineering and Research Institute (BAW) departmental research and development program. The dataset is available for download through the BAW-Datenrepository (https://doi.org/10.48437/02.2021.K.9900.0001).

## 8 References

Ashley, G. M.: Classification of Large-Scale Subaqueous Bedforms: A New Look at an Old Problem-SEPM Bedforms and Bedding Structures. In: Journal of Sedimentary Research 60 (1), 160–172, https://10.2110/jsr.60.160, 1990.

Bennett, S. J.; Best, J. L.: Mean flow and turbulence structure over fixed, two-dimensional dunes: implications for sediment transport and bedform stability. In: Sedimentology 42, 491–513, checked on 5/10/2019, 1995.

Best, J.: The fluid dynamics of river dunes. A review and some future research directions. In: J. Geophys. Res. 110 (F4), https://10.1029/2004JF000218, 2005.

Best, J.; Kostaschuk, R.: An experimental study of turbulent flow over a low-angle dune. In: J. Geophys. Res. 107 (C9), 318, https://10.1029/2000JC000294, 2002.

Bundesanstalt für Wasserbau: Das Schwebstoffmessprogramm an Weser, Elbe und Ems 2009-2011. Messbericht, Internal report, unpublished, 2016.

Bundesanstalt für Wasserbau: Laborversuche in einer Strömungsrinne mit skalierter Modelldüne (EbbSF) [Data set], https://doi.org/10.48437/02.2021.K.9900.0001, 2021.

Cisneros, J.; Best, J.; van Dijk, T.; Almeida, R. P. de; Amsler, M.; Boldt, J. et al.: Dunes in the world's big rivers are characterized by low-angle lee-side slopes and a complex shape. In: Nat. Geosci. 13 (2), 156–162, https://10.1038/s41561-019-0511-7, 2020.

Dalrymple, R. W.; Rhodes, R. N.: Estuarine Dunes and Bars. In: G.M.E. Perillo (Ed.): Developments in Sedimentology. Geomorphology and Sedimentology of Estuaries, 53, 359–422, 1995.

Engel, P.: Length of flow separation over dunes. In: Journal of the Hydraulics Division, ASCE 107, 1133–1143, 1981.

Fernandez, R.; Best, J. L.; López, F.: Mean flow, turbulence structure, and bed form superimposition across the ripple-dune transition. In: Water Resour. Res. 42 (5), 169, https://10.1029/2005WR004330, 2006.

Goring, D. G.; Nikora, V. I.: Despiking Acoustic Doppler Velocimeter Data. In: J. Hydraul. Eng. 128 (1), 117–126, https://10.1061/(ASCE)0733-9429(2002)128:1(117), 2002.

Herrling, G.; Becker, M.; Lefebvre, A.; Zorndt, A.; Krämer, K.; Winter, C.: The effect of asymmetric dune roughness on tidal asymmetry in the Weser estuary. In: Earth Surf. Process. Landforms 46 (11), 2211–2228, https://10.1002/esp.5170, 2021.

inphoris GmbH; smile consult GmbH: Airborne Laser-Scanner-Befliegungen der Unter- und Außenweser 2012 bis 2015, Abschlussbericht Bearbeitungsjahr 2012, 2014.

Kostaschuk, R.; Best, J.: Response of sand dunes to variations in tidal flow. Fraser Estuary, Canada. In: J. Geophys. Res. 110 (F4), https://10.1029/2004JF000176, 2005.

Kostaschuk, R.; Villard, P.: Flow and sediment transport over large subaqueous dunes. Fraser River, Canada. In: Sedimentology 43 (5), 849–863, https://10.1111/j.1365-3091.1996.tb01506.x, 1996.

Kwoll, E.; Venditti, J. G.; Bradley, R. W.; Winter, C.: Flow structure and resistance over subaqueous high- and low-angle dunes. In: J. Geophys. Res. Earth Surf. 121 (3), 545–564, https://10.1002/2015JF003637, 2016.

Lefebvre, A.: Three-Dimensional Flow Above River Bedforms. Insights From Numerical Modeling of a Natural Dune Field (Río Paraná, Argentina). In: J. Geophys. Res. Earth Surf. 124 (8), 2241–2264, https://10.1029/2018JF004928, 2019.

Lefebvre, A.; Herrling, G.; Becker, M.; Zorndt, A.; Krämer, K.; Winter, C.: Morphology of estuarine bedforms, Weser Estuary, Germany. In: Earth Surf. Process. Landforms 47 (1), 242–256, https://10.1002/esp.5243, 2021.

Lefebvre, A.; Herrling, G.; Zorndt, A.; Krämer, K.; Becker, M.; Winter, C.: Tidal bedforms dynamics, Weser River, Germany. EGU General Assembly 2020, Online, 4–8 May 2020, EGU2020-13499, https://10.5194/egusphere-egu2020-13499, 2020.

Lefebvre, A.; Paarlberg, A. J.; Ernstsen, V. B.; Winter, C.: Flow separation and roughness lengths over large bedforms in a tidal environment: A numerical investigation. In: Continental Shelf Research 91, 57–69, https://10.1016/j.csr.2014.09.001, 2014a.

Lefebvre, A.; Paarlberg, A. J.; Winter, C.: Flow separation and shear stress over angle-of-repose bed forms. A numerical investigation. In: Water Resour. Res. 50 (2), 986–1005, https://10.1002/2013WR014587, 2014b.

Lefebvre, A.; Paarlberg, A. J.; Winter, C.: Characterising natural bedform morphology and its influence on flow. In: Geo-Mar Lett 36 (5), 379–393, https://10.1007/s00367-016-0455-5, 2016.

Lefebvre, A.; Winter, C.: Predicting bed form roughness. The influence of lee side angle. In: Geo-Mar Lett 36 (2), 121–133, https://10.1007/s00367-016-0436-8, 2016.

Nelson, J. M.; McLean, S. R.; Wolfe, S. R.: Mean Flow and Turbulence Fields Over Two-Dimensional Bed Forms. In: Water Resour. Res. 29 (12), 3935–3953, 1993.

Nortek: The Comprehensive Manual for Velocimeters. Vector, Vectrino, Vectrino Profiler, https://support.nortekgroup.com/hc/en-us/articles/360029839351-The-Comprehensive-Manual-Velocimeters, 2018.

Paarlberg, A. J.; Dohmen-Janssen, C. M.; Hulscher, S. J. M. H.; Termes, P.: A parameterization of flow separation over subaqueous dunes. In: Water Resour. Res. 43 (12), 161, https://10.1029/2006WR005425, 2007.

Parsons, D. R.; Best, J. L.; Orfeo, O.; Hardy, R. J.; Kostaschuk, R. A.; Lane, S. N.: Morphology and flow fields of three-dimensional dunes, Rio Paraná, Argentina. Results from simultaneous multibeam echo sounding and acoustic Doppler current profiling. In: J. Geophys. Res. 110 (F4), https://10.1029/2004JF000231, 2005.

Venditti, J. G.: Bedforms in Sand-Bedded Rivers. In: John F. Shroder (Ed.): Treatise on geomorphology. London, Waltham, MA: Academic Press, 137–162, https://10.1016/B978-0-12-374739-6.00235-9, 2013.

Winter, C.; Lefebvre, A.; Becker, M.; Ferret, Y.; Ernstsen, V. B.; Bartholdy, J. et al.: Properties of active tidal bedforms. In: Thierry Garlan (Ed.): Marine and River Dune Dynamics. North Wales, UK, 2016.

WSV: Gewässerkundliches Informationssystem der Wasserstraßen- und Schifffahrtsverwaltung des Bundes, http://www.pegelonline.wsv.de/gast/stammdaten?pegelnr=4970030, 2020.